

Optical Near Field Phenomena in Planar and Structured Organic Solar Cells

M. Niggemann^{a,b}, T. Ziegler^a, M. Glatthaar^b, M. Riede^a, B. Zimmermann^b and A. Gombert^a

^a Fraunhofer Institute for Solar Energy Systems (ISE), Heidenhofstr. 2, 79110 Freiburg, Germany;

^b Material Research Center Freiburg (FMF), Stefan-Meier-Str. 21, 79104 Freiburg, Germany

ABSTRACT

One key problem in optimizing organic solar cells is to maximize the absorption of incident light and to keep the charge carrier transport paths as short as possible in order to minimize transport losses. The large versatility of organic semiconductors and compositions requires specific optimization of each system. We investigate two model systems, the MDMO-PPV:PCBM blend and the P3HT:PCBM blend. Due to the small thickness of the functional layers in the order of several ten nanometers, coherent optics has to be considered and therefore interference effects play a dominant role. The influence of the thickness of the photoactive layer on the light absorption is investigated and compared with experimental data. The potential of an optical spacer which is introduced between the aluminium electrode and the photoactive layer to enhance the light harvesting is evaluated by optical modelling. Optical modelling becomes more complex for novel solar cell architectures based on nanostructured substrates. Exemplary optical simulations are presented for a nanoelectrode solar cell architecture.

Keywords: organic solar cell, light trapping, nano electrode, optical modelling, optical spacer

1. INTRODUCTION

Organic solar cells have become a very attractive research topic, as they have the potential for low cost production and are expected to give rise to new applications due to their mechanical flexibility. The efficiency has been doubled during the last four years, reaching values close to 5%.¹ Together with the reported longterm stability, the goal of commercialization of first organic solar cell products is within reach.² A promising concept of an organic solar cell is the so called bulk heterojunction solar cell.³ The most widely investigated organic semiconductors for organic solar cells are the conjugated polymers poly-3(hexyl-thiophene)(P3HT) and poly-[2-(3,7-dimethyloctyloxy)-5-methyloxy]-para-phenylene-vinylene (MDMO-PPV) serving as electron donor component and [6,6]-phenyl C61 - butyric acid methyl ester (PCBM, a C₆₀-derivative) as electron acceptor.⁴ The major limitations are still the too large optical bandgap of the organic semiconductors and the small charge carrier mobilities. Therefore, the thickness of the photoactive layer is limited to 100 nm up to 300 nm. The architecture of most organic electronic devices is planar. The devices are fabricated on indium tin oxide (ITO) coated on a glass- or polymer substrate serving as a transparent electrode. Subsequently the organic layers, poly(3,4-ethylene-dioxy-thiophene)-poly(styrene sulfonate) (PEDOT:PSS), serving as anode and the photoactive blend are deposited from solution.

Implementing micro- and nanopatterned structures in these organic electronic devices offers the possibility to optimize devices, or even to create novel devices architectures. Optical modelling is assumed to be essential for proper dimensioning of the structures. The thickness of the substrate of most organic solar cell architectures exceeds the coherence length of the sunlight, whereas the thickness of the photoactive and passive layers is smaller than the wavelength of the incident light. Therefore, incoherent and coherent optics have to be considered. A very versatile method to calculate the optical near field in corrugated layer systems, as well as the resulting far field is the so called Rigorous Coupled Wave Analysis (RCWA).^{5,6} We applied this method to investigate the optical near field in the planar solar cell with the two photoactive composites MDMO-PPV:PCBM and P3HT:PCBM. In particular, the influences of the thickness of the photoactive layer and the effect of an optical spacer on the light absorption are studied.

Further author information: E-mail: Michael.Niggemann@ise.fraunhofer.de, Telephone: +049 (0)761 2034798

The optical near field phenomena were studied for a novel device architectures based on nanoelectrodes, as well. Interdigital buried nanoelectrodes form a comb-like array of vertically orientated electrodes embedded in the photoactive layer. In principle, this architecture follows the requirement of a geometric decoupling of the charge carrier transport from the light absorption. As the dimensions of the structures are below the wavelength of the incident light, optical near field phenomena have to be taken into account for modelling. Two polarisations of the incident light - transversal electric (TE) and transversal magnetic (TM) have to be considered.

2. OPTICAL CONSTANTS OF ORGANIC ABSORBERS AND BLENDS

Optical constants of the most widely investigated organic semiconductor donor components MDMO-PPV and P3HT and PCBM as acceptor including the optical constants for the respective blends are presented here. The optical constants for PCBM and the P3HT/PCBM blend (weight ratio 6:5) in tetraline were determined on the basis of spectroscopic ellipsometry and transmittance measurements. The normal transmission spectra were taken with a Perkin Elmer Lambda 40 UV/VIS Spektrometer. The dielectric function was fitted in the spectral range between 750 nm and 1000 nm using a commercial software Simulay (version 1.0 Optosol GbR). The ellipsometry measurement were made using a rotating-compensator-ellipsometer manufactured by J.A. Woollam (type M-2000U). The measurements were performed at angles in the range between 50° and 70° and the data acquisition and fitting was done using the software WVase (Windows Variable Angle Spectroscopic Ellipsometry). In the non absorbing region between 750 nm and 1000 nm a Cauchy model was used for determination of the real part of the refractive index. Optical constants for the MDMO-PPV/PCBM system (solvent chlorobenzene, weight ratio 1:4) and the PEDOT A14083 were determined by Hoppe et al.⁷ The optical constants of the used organic semiconductors and semiconductor blends are shown in figure 1.

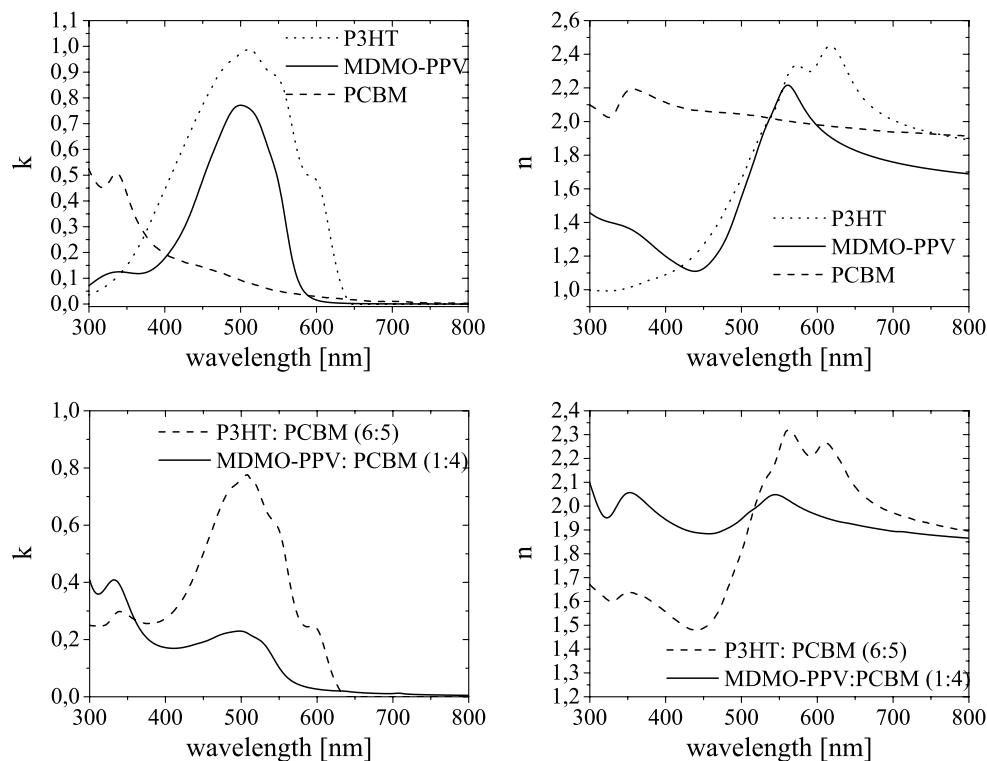


Figure 1. Optical constants of the investigated materials. Upper left and right: Imaginary and real part of the complex dielectric function of the pristine semiconductors PCBM, MDMO-PPV and P3HT. Lower left and right: Imaginary and real part of the dielectric function of the semiconductor blends MDMO-PPV:PCBM (1:4) and P3HT:PCBM (6:5). The optical constants for MDMO-PPV and MDMO-PPV:PCBM were determined by Hoppe et al.⁷

The most important differences in the imaginary part of the refractive indices of the pristine conjugated polymers are the stronger absorption and wider absorption spectrum of P3HT in comparison to MDMO-PPV. Especially the extended absorption edge close to 650 nm causes the improved harvesting of the sunlight of this material. The highest absorption coefficient of PCBM is in the short wavelength range below 400 nm. The two blends differ strongly in their absorption strengths in the visible range and in the ratios between PCBM- and conjugated polymer peak heights. This can be traced back to the different optimum weight ratios of the two blends. A weight ratio of 1:4 turned out to result in the most efficient MDMO-PPV:PCBM based solar cells. The high fraction of PCBM is required in order to allow the formation of nanocrystals of neat C60 which is essential to avoid recombination losses and as a consequence, causes an optical dilution of the absorber composite. Exciton splitting and electron transport in the P3HT:PCBM blend is sufficiently efficient at lower PCBM content (weight ratio 6:5) and thus the absorptivity of this donor-acceptor composite is significantly stronger. The slope of the absorption edges of these two systems strongly influences the effect of light trapping structures.

3. OPTICAL MODELLING

The spectral reflectance, transmittance and absorptance and the spatial distribution of the optical near-field inside the thin film system are modelled. From the spectral absorptance in the distinct layers of the device, the charge generation in the active layer and the absorption losses in the adjacent films (ITO, PEDOT, aluminium) can be derived. These calculations are compared with absorption- and spectral response measurements. From spectral weighting of the absorptance in the active layer with the spectrum of the incident light, the short-circuit current density is calculated for a given internal quantum efficiency.

The planar organic solar cell, consisting mainly of a substrate carrying a thin film system, has to be described with coherent optics as well as with incoherent optics. As the coherence length of the sunlight is about 800 nm,⁸ the 1 mm thick glass substrate has to be treated incoherently whereas for the thin film system coherent description of the optics is mandatory. Since the thickness of a thin film system of several hundred nanometers is much smaller than the wavelength of the incident light, wave optics have to be considered. The calculations of the absorptance in distinct layers were performed by Rigorous Coupled Wave Analysis (RCWA), a method which was implemented for describing near-field phenomena at corrugated interfaces.^{5,6,9,10} The optical modelling of other solar cell architectures like the micropillar solar cell and diffraction gratings for light trapping is presented elsewhere.^{11,12}

3.1. Optical modelling of planar solar cells

The set-up of the planar organic solar cell is recalled here. An ITO (indium tin oxide) coated glass or plastic substrate is coated with a conjugated conductive polymer named PEDOT:PSS forming the p-contact. Subsequently the photoactive layer is spin coated from a solution. The cathode is realised by an evaporated aluminium electrode. The semiconductor/aluminium interface can be improved by introducing a thin lithium fluoride layer (nominal thickness 0.6 nm) resulting in a better fill factor and hence higher efficiencies.¹³ A variation of the blend layer thickness and the introduction of an optical spacer is investigated for the two organic semiconductor composites MDMO-PPV:PCBM and P3HT:PCBM.

3.1.1. Variation of the Absorber Thickness

The absorptance in the photoactive layer of the solar cell will be modelled here depending on its thickness whereas the thicknesses of the ITO- and the PEDOT-layers were kept constant. The P3HT:PCBM absorber serves as a model system here, distinct properties of the MDMO-PPV:PCBM blend are shown for comparison. The complex behaviour of the spectral absorptance in the distinct layers which can be observed when increasing the thickness of the photoactive layer can be traced back to interference effects. The spectral absorptance of the whole solar cell (P3HT:PCBM) is shown in figure 2 (left). The thickness of the photoactive layer is varied between 100 nm and 200 nm. The most significant features are, first, an increase of the absorption in the wavelength range between 550 nm and 630 nm and secondly, a shifting of a local absorption minimum from 370 nm up to 430 nm whereas the absorption maximum at 500 nm remains more or less unaffected. The first effect causes a significant increase of the absorption in the photoactive layer (not shown here) and therefore an increase of the photocurrent. The second effect is that the local minimum shifts linearly with the thickness of the photoactive

layer (figure 2 (right)). This behaviour is expected for thin film systems and can be used for a relatively precise determination of the film thickness without the necessity of quantitative absorption measurements or destructive thickness measurement methods.

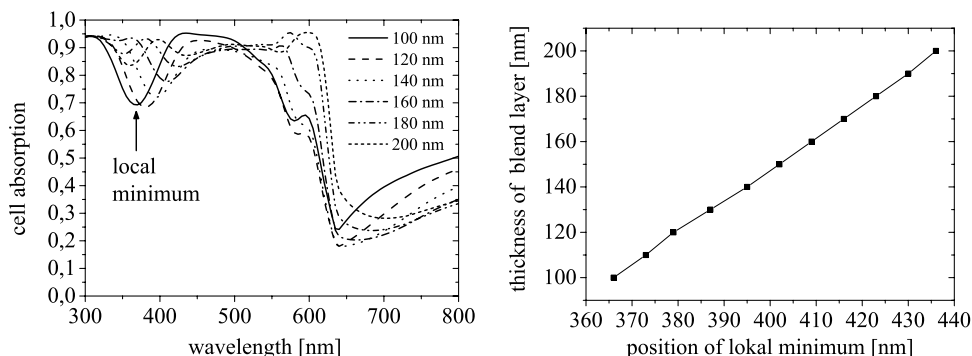


Figure 2. Left: Calculated spectral absorption of an organic solar cell with a P3HT:PCBM (6:5) blend layer of varying thickness. Right: Position of the first local absorption minimum depending on the thickness of the photoactive layer.

An estimate of the maximum photocurrent that can be extracted from the solar cell can be made for a given internal quantum efficiency under consideration of the solar AM 1.5 spectrum. We assume an internal quantum efficiency of unity. Hence, only optical losses and the light absorption in the photoactive layer are taken into account and recombination processes are excluded. The short-circuit current is plotted versus the thickness of the active polymer film (figure 3).

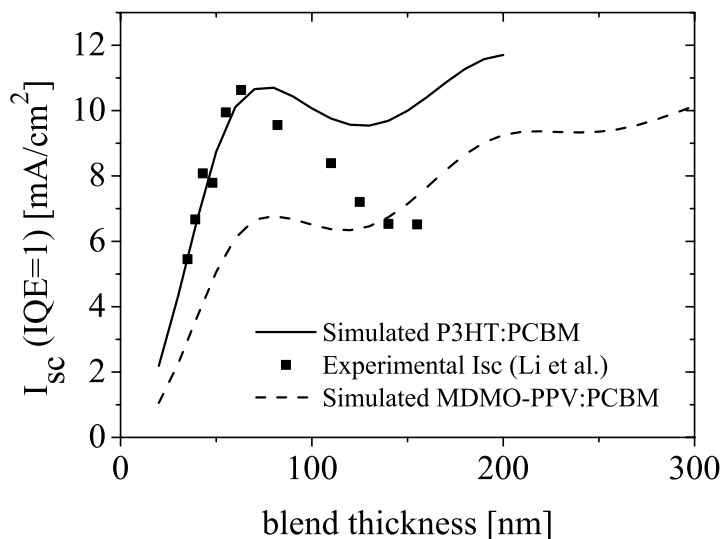


Figure 3. Calculated short-circuit current for different thicknesses of the two types of active layers assuming an internal quantum efficiency of unity. The measured short circuit current densities are according to the investigations on P3HT:PCBM solar cells published by Li et al..¹⁴

Li et al. investigated the influence of the short circuit current with respect to the thickness of the P3HT:PCBM blend layer.¹⁴ A good agreement can be observed between these measurements and the optical simulations up

to a film thickness of 60 nm. These results and the investigations on the loss mechanisms by Schilinsky et al.⁴ give a strong evidence for the high internal quantum efficiency of such devices for thin layers. Exemplary absorption measurements and optical simulations of the solar cells are presented in figure 4 (left). Thicknesses of 160 nm and 190 nm for the photoactive layer can be derived from the simulations. The measured spectral external quantum efficiencies of these devices follow the signature of the modelled blend absorption but are significantly smaller, indicating electrical losses for such thick cells (figure 4(right)).

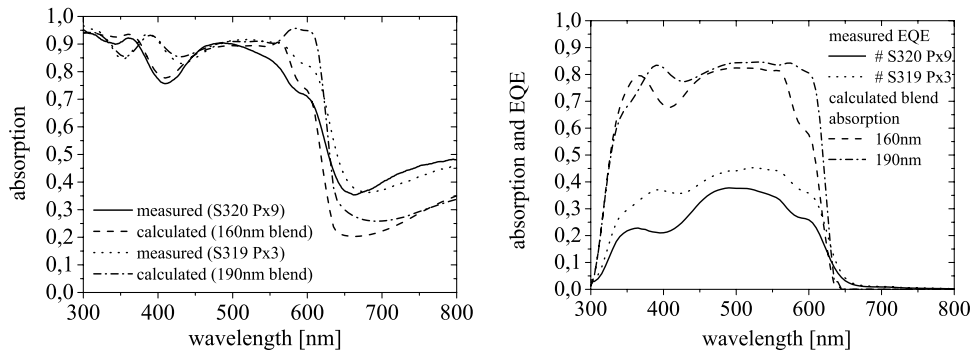


Figure 4. Left: Calculated and measured spectral absorption of two exemplary organic solar cells with a P3HT:PCBM (6:5) blend layer of varying thickness. Right: Calculated blend absorption and measured external quantum efficiency (EQE) of the same two cells.

3.1.2. Widegap Layer

A strong decay of the light intensity can be observed in optical simulations (not shown here) at the blend/metal interface over a broad range of wavelengths. This can be explained by the high conductivity of the metal. From the dispersion relation, it can be concluded, that the oscillation of free electrons is phase shifted by 180°. This leads to the formation of a node at the metal interface due to destructive interference.¹⁵ As a consequence, less charge carriers will be created in the vicinity of the metal electrode, but electrons have to travel through this region in order to arrive at the cathode. The introduction of a highly conductive so called wide gap layer or optical spacer should allow to minimize transport losses. This approach has been investigated by Drechsel et al. for evaporated small molecule organic solar cells.¹⁶ The thickness of the photoactive layer of such devices is limited to 30 nm due to the small charge carrier mobilities in the semiconductor composite. The introduction of such a wide gap layer in organic bulk heterojunction solar cells spin cast from solution was presented by Ma et al.¹ TiO_x was identified to serve as a good electron acceptor and is at the same time sufficiently transparent in the desired wavelength range ($E_g \approx 3.2\text{eV}$). As a result, an almost doubling of the monochromatic EQE at 500 nm was observed which was attributed to the presence of the TiO_x optical spacer. The overall device efficiency under AM1.5 illumination was increased by 40%. It has to be noted, that only 10% increase of the short circuit current was observed besides a significant improvement of the V_{oc} and FF. Therefore, the major contribution of the TiO_x layer is due to an improvement of the electronic interface, rather than due to an increase of the light absorption.

The influence of a TiO_2 optical spacer with varying thickness on the absorption in the photoactive layer is modelled for large variation of the thickness of the photoactive layer. Two types of photoactive layers are investigated, a P3HT:PCBM blend (6:5 by weight) and a MDMO-PPV:PCBM blend (1:4 by weight) (figures 5).

Upon the introduction of the optical spacer, the position of the local maximum of the short circuit current is shifted towards a smaller thickness of the photoactive layer. At the same time, the maximal short circuit current (height of the first local maximum) decreases with increasing thickness of the optical spacer. This can be explained by small absorptions in the optical spacer which do not contribute to a charge carrier generation. By introducing a 20 nm thick optical spacer, the calculated short circuit current of a P3HT:PCBM device shows

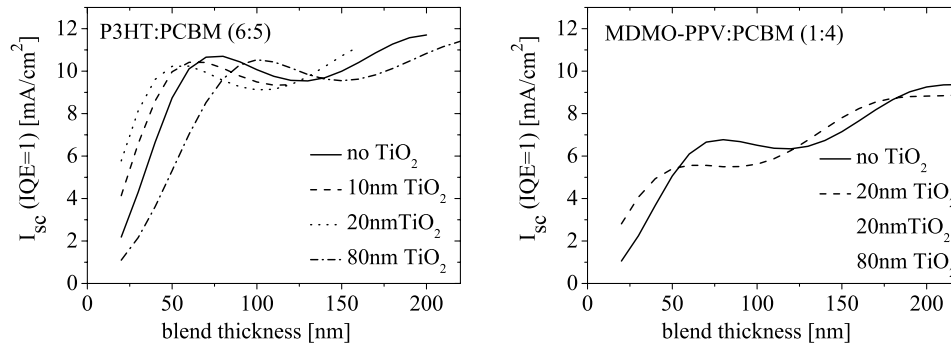


Figure 5. Influence of a TiO_2 spacer layer inbetween aluminium cathode and photoactive layer on the calculated short-circuit current for different thicknesses of the photoactive layer (Assuming an internal quantum efficiency of unity). Left: P3HT:PCBM blend (6:5 by weight). Right: MDMO-PPV:PCBM blend (1:4 by weight).

a relative increase between 0% up to 60% for a decreasing thickness of the photoactive layer ranging between 60 nm and 20 nm . A contribution of the optical spacer to an increased absorption is calculated for an absorber thickness exceeding 120 nm up to a certain value which has not been calculated here. The device with the MDMO-PPV:PCBM blend shows a similar behaviour (figure 5 (right)). The critical thickness of the photoactive layer is 55 nm . A 20 nm thick optical spacer will enhance the light absorption in photoactive layers below a thickness of 55 nm and within an interval between 120 nm and 180 nm . Summing up, optical spacers are of largest benefit for photoactive layers whose thickness is limited by transport losses to values significantly below 50 nm . Nevertheless, the absorption in thicker photoactive layers can be optimized by 5% to 10% by introducing an optical spacer.

4. INTERDIGITAL NANOELECTRODES

Buried nanoelectrodes are vertically orientated electrodes embedded in the photoactive layer of the solar cell. The substitution of both planar electrodes by buried nanoelectrodes results in an interdigital electrode set-up (figure 6).

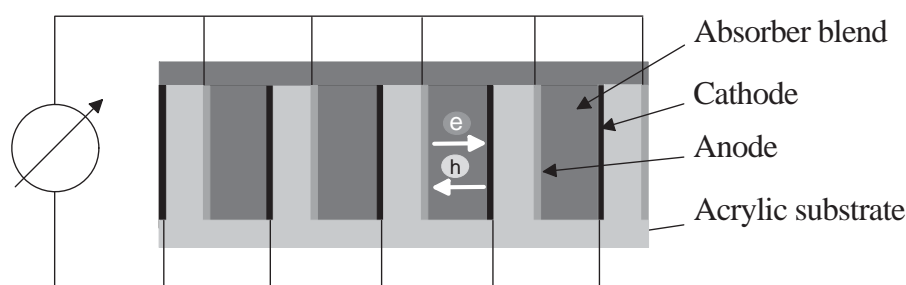


Figure 6. Concept of interdigital buried nanoelectrodes.

The dimensions of the buried nanoelectrodes are comparable to the thickness of the organic films. The period of the microstructure ($\Lambda = 720 \text{ nm}$) is in the range of the wavelength of the incident light. In principle, this architecture follows the requirement of separating the light absorption from the charge carrier transport. Hence, the effective thickness of the absorber can be increased while keeping the distance of the electrodes small enough for an efficient charge extraction. However, technological limitations with respect to the aspect ratio of the structures have to be considered. In contrast to the planar solar cell architecture based on an ITO substrate, both electrodes are deposited prior to the application of the photoactive film. This can be of advantage for the device preparation because no vacuum deposition step is required after the deposition of the organic compounds. Another feature is the absence of a highly reflecting back electrode. This makes semitransparent applications possible. The interface formation is an important issue. Suitable contacts with high selectivity are under investigation. As the dimensions of these structures are in the range of the wavelength of light, near-field optics plays an important role.

The experimental results are summed up as follows, details are presented elsewhere.¹⁷ The substrate for buried nanoelectrodes is made by replication of holographically created structures into an acrylic UV curable photopolymer. The dimensions of the microstructure are a lamellae period of 720 nm , a depth of approximately 400 nm and a cavity width of 400 nm . Two separated metal electrodes form an interdigital electrode array. The electrode materials have to provide good contacts for the organic semiconductor. One prerequisite is the matching of the electrode workfunction to the respective quasi Fermi potentials of the semiconductor. First experiments were carried out with a titanium and a gold electrode serving as cathode and anode respectively. An exemplary nanoelectrode structure filled with the photoactive material is shown in figure 7.

Interdigital nanoelectrodes can be realized on small areas (5 mm^2) with sufficiently large parallel resistance. The proof of principle has been given with first devices ($FF = 25\%$, $I_{SC} = 0.5 \text{ mA/cm}^2$, $U_{OC} = 380 \text{ mV}$). The

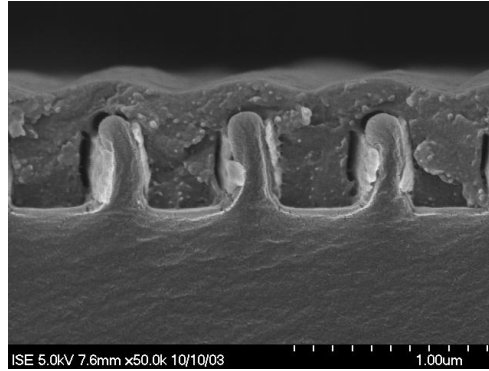


Figure 7. Nanoelectrode structure filled with the photoactive material.

rectification of the device is rather low. We attribute this effect to an insufficient selectivity of the gold electrode for the respective charge carriers. As a consequence, the hole contact needs to be optimized in order to allow an efficient charge collection.

4.1. Optical modelling

The dimensions of the nanostructure are determined by the charge carrier mobilities. From the planar solar cells with a P3HT:PCBM-absorber it is known that an absorber thickness of 300 nm can be realised. Therefore, a lamellar structure with a period of 720 nm and with a cavity width of 430 nm is assumed to allow a charge extraction. The dimension of the structure is in the range of the wavelength and therefore optical near-field calculations were performed.

A simplified lamellar structure with a period of 720 nm and a cavity depth and width of 1000 nm and 430 nm respectively was chosen for the simulations. The lamellar metal electrodes were simulated by solid aluminium. The calculated spectral absorptance for both, TE- and TM-polarisation is shown in figure 8.

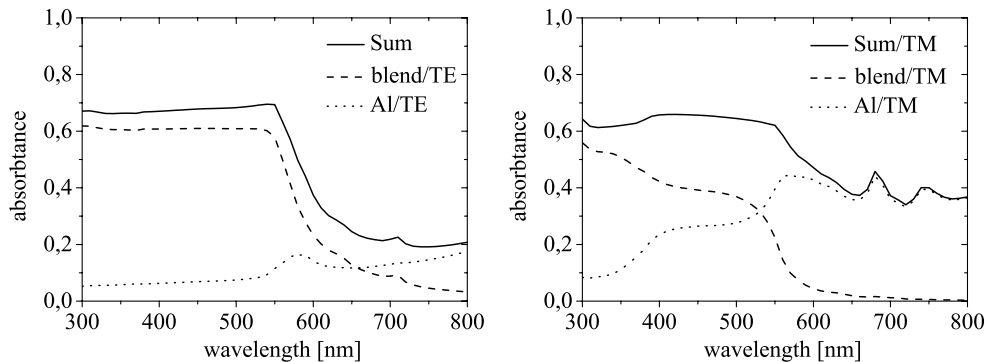


Figure 8. RCWA simulation of the spectral absorptance in the lamellar structures ($\Lambda = 720$ nm, depth=1 μ m, cavity-width=430 nm) filled with the active polymer (MDMO-PPV/PCBM, 1:4). Left: Calculations for TE-polarised light. Right: Calculations for TM-polarised light.

The calculations show a saturation of the blend absorptance in TE-polarisation at about 60% at wavelengths up to 550 nm (figure 8 (left)). This is in accordance to the ratio of the cavity width and the structure period. TM-polarised light shows a rather complex absorption characteristic (figure 8 (right)). A large fraction of the light is absorbed in the aluminium and as a result the light absorption in the blend decreases. At wavelengths exceeding 600 nm, the absorption is dominated by losses in the metal.

The simulated stronger absorption in TM-polarisation in comparison to the TE-polarisation shall be investigated in detail here. Examples of optical near-field calculations based on RCWA for TE- and TM-polarisation are shown in figure 9. The spatial distribution of the light intensity inside the polymer filled cavity differs significantly for the two polarisations. In contrast to the increased field intensities in the centre of the cavity for TE-polarisation, an opposite tendency can be observed for TM-polarised light. High field intensities are observed close to the metal interface.

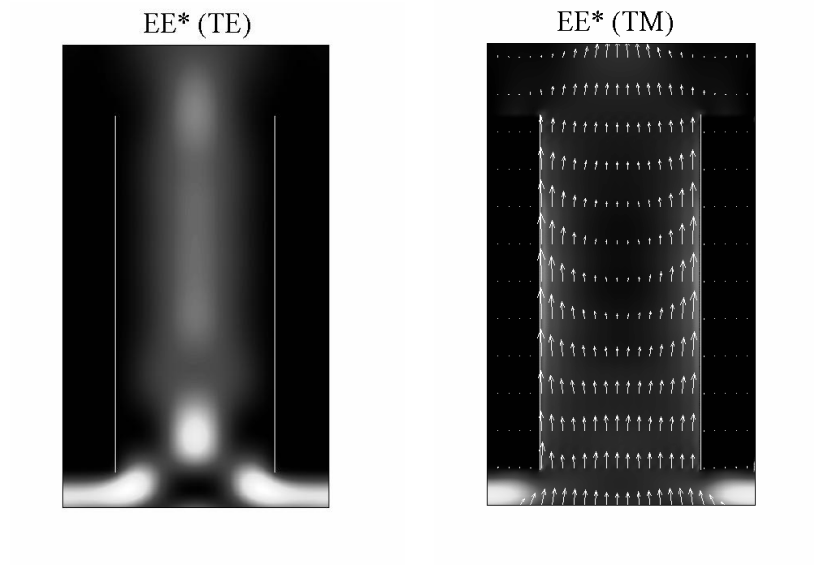


Figure 9. Simulation of the optical near-field in a lamellar aluminium structure with a period of 720 nm and a depth and width of the cavities of 1000 nm and 430 nm respectively filled with active polymer (normal incidence, $\lambda = 500\text{ nm}$). Left: TE-polarisation. Right: TM-polarisation with Poynting vectors.

The Poynting vectors oriented nearly parallel to the metal surface indicate the propagation direction. High field intensities in TM-polarisation close to the metal surface with a propagation direction parallel to the metal surface result in an electric field vector oriented perpendicular to the metal surface. It can be shown that this arrangement results in enhanced radiation losses in the metal layer and therefore cause the losses for TM polarised light.

5. CONCLUSIONS AND OUTLOOK

The light absorption in organic solar cells is dominated by interference effects. The widely investigated photoactive composites for organic solar cells, MDMO-PPV:PCBM and P3HT:PCBM differ strongly in their light absorption properties. The imaginary part of the dielectric function of the P3HT:PCBM blend is up to four times larger (at 500 nm) than for the MDMO-PPV:PCBM blend. This is caused by the higher absorptivity of the pristine P3HT and by the higher fraction of this component in the organic semiconductor blend (55% instead of 20%). The absorption spectra of the solar cells shows a significant signature caused by the interference. The position of local minima scales linearly with the thickness of the photoactive layer and can therefore be used for an efficient monitoring of the production processes of organic solar cells. Comparative investigations of the calculated light absorption in the photoactive layer of P3HT:PCBM devices and measurements of the short circuit current indicate an internal quantum efficiency close to 1 for layer a thickness below 60 nm . Optical calculations show that the introduction of an optical spacer inbetween the aluminium cathode and the photoactive layer is beneficial for distinct thickness intervals of the photoactive layer. The absorption can be doubled for very thin

layers (30 nm for P3HT:PCBM and 20 nm for MDMO-PPV:PCBM for a 20 nm TiO_2 spacer). The benefit in absorption at larger thickness of the photoactive layer is significantly smaller, ranging between 5% and 10%.

Interdigital buried nanoelectrodes are still at an early stage of the investigations. Optical modelling was made for a MDMO-PPV:PCBM blend. Two loss mechanisms have been identified as (i) area losses due to the filling factor of the photoactive nanocavities and (ii) absorption losses in the metal electrode for TM-polarised light. One approach to reduce the absorption losses would be the substitution of the metal by a dielectric material which serves as a good contact and is sufficiently conductive.

ACKNOWLEDGMENTS

Special thanks to Autotype Ltd, Wantage England for the replication of the microstructures.

REFERENCES

1. W. L. Ma, C. Y. Yang, X. Gong, K. Lee, and A. J. Heeger. Thermally stable, efficient polymer solar cells with nanoscale control of the interpenetrating network morphology. *Advanced Functional Materials*, 15(10):1617–1622, 2005.
2. R. DE BETTIGNIES, J. Leroy, and M. S. C. Firon. Study of p3ht:pcbm bulk heterojunction solar cells : influence of components ratio and of the nature of electrodes on performances and lifetime. *Spie Optics and Photonics*, Jul 2005.
3. S. E. Shaheen, C. J. Brabec, N. S. Sariciftci, F. Padinger, T. Fromherz, and J. C. Hummelen. 2.5 *Applied Physics Letters*, 78(6):841–843, 2001.
4. P. Schilinsky, C. Waldauf, and C. J. Brabec. Recombination and loss analysis in polythiophene based bulk heterojunction photodetectors. *Applied Physics Letters*, 81(20):3885–3887, 2002.
5. M. G. Moharam and T. K. Gaylord. Rigorous coupled wave analysis of planar diffraction gratings. *Journal of the Optical Society of America A-Optics Image Science and Vision*, 71:811–818, 1981.
6. P. Lalanne and M. P. Jurek. Computation of the near-field pattern with the coupled-wave method for transverse magnetic polarization. *Journal of Modern Optics*, 45(7):1357–1374, 1998.
7. H. Hoppe, N. S. Sariciftci, and D. Meissner. Optical constants of conjugated polymer/fullerene based bulk-heterojunction organic solar cells. *Molecular Crystals and Liquid Crystals*, 385:233–239, 2002.
8. B. E. A. Saleh and M. C. Teich. *Fundamentals of Photonics*. Wiley, New York, 1991.
9. M. G. Moharam and T. K. Gaylord. Diffraction analysis of dielectric surface-relief gratings. *Journal of the Optical Society of America*, 72(10):1385–1392, 1982.
10. P. Lalanne and G. M. Morris. Highly improved convergence of the coupled-wave method for transversal magnetic polarization. *Journal of the Optical Society of America A-Optics Image Science and Vision*, 13(4):779–784, 1996.
11. M. Niggemann, M. Glatthaar, P. Lewer, C. Mller, J. Wagner, and A. Gombert. Functional micropism substrate for organic solar cells. *Thin Solid Films*, 2006.
12. M. Niggemann, M. Glatthaar, A. Gombert, A. Hinsch, and V. Wittwer. Diffraction gratings and buried nano-electrodes - architectures for organic solar cells. *Thin Solid Films*, 451-452:619–623, 2004.
13. C. J. Brabec, S. E. Shaheen, C. Winder, N. S. Sariciftci, and P. Denk. Effect of lif/metal electrodes on the performance of plastic solar cells. *Applied Physics Letters*, 80(7):1288–1290, 2002.
14. G. Li, V. Shrotriya, Y. Yao, and Y. Yang. Investigation of annealing effects and film thickness dependence of polymer solar cells based on poly(3-hexylthiophene). *Journal of Applied Physics*, 98(043704), 2005.
15. E. Hecht. *OPTIK*. Number Book in 1. Addison-Wesley Publishing Company, 3. korrigierter nachdruck edition, 1974.
16. J. Drechsel, B. Mannig, F. Kozlowski, M. Pfeiffer, K. Leo, and H. Hoppe. Efficient organic solar cells based on a double p-i-n architecture using doped wide-gap transport layers. *Applied Physics Letters*, 86(24), 2005.
17. M. Niggemann, M. Glatthaar, D. Ruf, M. Riede, C. Mueller, B. Zimmermann, and A. Gombert. Functional substrates for flexible organic photovoltaic cells. *SPIE Optics and Photonics 31. 07-4-08. 2005 San Diego, California USA*, Proceedings, 2005.